

# Synthesis and Reactivity of (N2P2)Ni Complexes Stabilized by a Diphosphonite Pyridinophane Ligand

Kei Fuchigami, Michael B. Watson, Giang N. Tran, Nigam P. Rath, and Liviu M. Mirica\*

Cite This: *Organometallics* 2021, 40, 2283–2289

Read Online

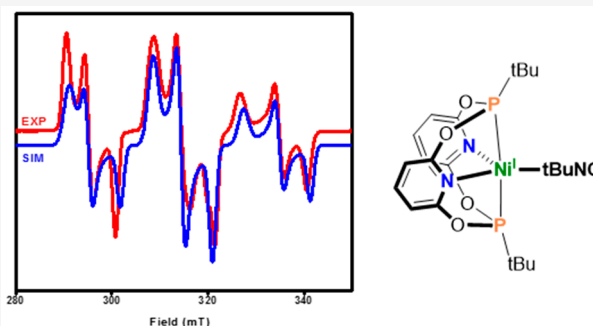
ACCESS |

Metrics & More

Article Recommendations

Supporting Information

**ABSTRACT:** A series of (N2P2)Ni<sup>II</sup> complexes (N2P2 = *P,P'*-ditertbutyl-2,11-diphosphonito[3.3](2,6)pyridinophane) stabilized by a modified tetradentate pyridinophane ligand containing two phosphonite groups were synthesized and characterized. Cyclic voltammetry (CV) studies revealed the accessibility of the Ni<sup>I</sup> oxidation state at moderate redox potentials for these Ni<sup>II</sup> complexes. *In situ* EPR, low-temperature UV–vis, and electrochemical studies were employed to detect the formation of Ni<sup>I</sup> species during the reduction of Ni<sup>II</sup> precursors. Furthermore, the [(N2P2)Ni<sup>I</sup>(CN*t*-Bu)](SbF<sub>6</sub>) complex was isolated upon reduction of the Ni<sup>II</sup> precursor with 1 equiv of CoCp<sub>2</sub> and was characterized by EPR and X-ray photoelectron spectroscopy (XPS). Finally, the (N2P2)Ni<sup>II</sup>Br<sub>2</sub> complex acts as an efficient catalyst for the Kumada cross-coupling of an aryl halide with an aryl or alkyl Grignard, suggesting that the N2P2 ligand can support the various Ni species involved in the catalytic C–C bond formation reactivity.



## INTRODUCTION

In addition to Pd-catalyzed transformations, Ni-based catalytic systems have recently been developed that can promote Negishi, Kumada, and Suzuki cross-coupling reactions.<sup>1–10</sup> Contrary to the extensively studied Pd-mediated transformations that employ diamagnetic intermediates, Ni has been found to undergo both one- and two-electron redox reactions leading to additional reaction pathways. Although there is evidence that Pd can also undergo similar redox reactions, Ni has been more commonly accepted to involve the +1 and +3 oxidation states in the aforementioned cross-coupling reactions.<sup>11–20</sup> The presence of these paramagnetic species has made the characterization of these reactive species more difficult,<sup>21–25</sup> yet a detailed understanding of these paramagnetic Ni complexes will lead to the development of more efficient and selective catalysts for Ni-mediated cross-coupling reactions.

In the past several years we have reported the isolation and characterization of mononuclear organometallic Ni<sup>III</sup> complexes stabilized by tetradentate <sup>R</sup>N<sub>4</sub> ligands (<sup>R</sup>N<sub>4</sub> = *N,N'*-dialkyl-2,11-diaza[3.3](2,6)pyridinophane, R = Me, <sup>i</sup>Pr, or <sup>t</sup>Bu) as well as its C-donor derivative <sup>R</sup>N<sub>3</sub>C<sup>−</sup> ligands (R = <sup>t</sup>Bu, *tert*-butyl, or neopentyl (Np)) that can undergo C–C and C–heteroatom bond formation reactions.<sup>26–36</sup> These results suggest that Ni<sup>III</sup> complexes are more common than previously anticipated; thus, it prompted us to now target the low-valent Ni<sup>I</sup> species using a slightly modified ligand system. Inspired by the many examples of PONOP-type pincer metal complexes,<sup>37–41</sup> we have developed the N- and P-donor

tetradentate ligand *P,P'*-ditertbutyl-2,11-diphosphonito[3.3](2,6)pyridinophane (N2P2) and investigated the redox properties and reactivity of its Ni complexes. Reported herein are the synthesis, characterization, and reactivity studies of a series of (N2P2)Ni complexes, including a rare [(N2P2)-Ni<sup>I</sup>(CN*t*-Bu)](SbF<sub>6</sub>) (**6**) complex. Interestingly, we have also observed that the (N2P2)Ni<sup>II</sup>Br<sub>2</sub> (**1**) complex can catalyze the Kumada cross-coupling of an aryl halide with an aryl or alkyl Grignard, suggesting that the N2P2 ligand can support the various Ni species that are involved in the catalytic C–C bond formation reactivity.

## EXPERIMENTAL DETAILS

**Reagents and Materials.** All manipulations were carried out under a nitrogen atmosphere using standard Schlenk and glovebox techniques if not indicated otherwise. All reagents for which the synthesis is not given were commercially available from Sigma-Aldrich, Fischer, or Strem and were used as received without further purification. Solvents were purified prior to use by passing through a column of activated alumina using an MBRAUN SPS. Ni(DME)Br<sub>2</sub> (DME = ethylene glycol dimethyl ether) was prepared according to a modified literature procedure.<sup>42</sup>

**Special Issue:** Organometallic Solutions to Challenges in Cross-Coupling

**Received:** January 2, 2021

**Published:** April 12, 2021



**Physical Measurements.**  $^1\text{H}$  (300.121 MHz) NMR spectra were recorded on a Varian Mercury-300 spectrometer. Solution magnetic susceptibility measurements were obtained by the Evans method<sup>43</sup> using coaxial NMR tubes at 293 K. Diamagnetic corrections were applied as previously described.<sup>44</sup> UV–vis spectra were recorded on a Varian Cary 50 Bio spectrophotometer and are reported as  $\lambda_{\text{max}}$  nm ( $\epsilon$ ,  $\text{M}^{-1} \text{cm}^{-1}$ ). The low-temperature UV–vis measurements were performed using a fiber-optic immersion probe (Hellma, path length 1 mm or 10 mm). EPR spectra were recorded on a JEOL JES-FA X-band (9.2 GHz) EPR spectrometer at 77 or 298 K. EPR spectra simulation and analysis were performed using Bruker WINEPR SimFonia program, version 1.25. ESI-MS experiments were performed using a Thermo FT or Bruker Maxis Q-TOF mass spectrometer with an electrospray ionization source. Elemental analyses were carried out by the Columbia Analytical Services Tucson Laboratory. Cyclic voltammetry (CV) experiments were performed with a BASi EC Epsilon electrochemical workstation or a CHI 660D Electrochemical Analyzer.

**Electrochemical Measurements.** Electrochemical-grade  $\text{Bu}_4\text{NClO}_4$  (Fluka) was used as the supporting electrolyte. Electrochemical measurements were performed in the  $\text{N}_2$ -filled glovebox or under a blanket of nitrogen, and the analyzed solutions were deaerated by purging with nitrogen. A glassy carbon disk electrode ( $d = 1.6$  mm) was used as the working electrode, and a Pt wire was used as the counter electrode. A Ag wire pseudoreference electrode or a Ag/0.01 M  $\text{AgNO}_3/\text{MeCN}$  electrode was used as the reference electrode. The nonaqueous reference electrode was calibrated against  $\text{Cp}_2\text{Fe}$  (Fc). **Caution!** Perchlorate salts are potentially explosive and should be handled with appropriate care only in small quantities.

**Synthesis of N2P2 Ligand.** 2,6-Dihydroxypyridine hydrochloride (Aldrich, 500 mg, 3.388 mmol) and 100 mL of THF was combined in a Schlenk flask equipped with a rubber septum. The solution was precooled. To the above mixture, *n*-butyl lithium (Aldrich 2.5 M in hexane, 4 mL, 10.00 mmol) was added dropwise while stirring. The reaction mixture was brought to room temperature and stirred for 1.5 h. After the solution became cloudy, a phosphine solution of *p,p*-dichloro-*tert*-butylphosphine (Aldrich 1.0 M in  $\text{Et}_2\text{O}$ , 3.2 mL, 3.227 mmol) in 100 mL of THF was prepared and added dropwise. The reaction mixture was further stirred for 24 h. The solvent was then removed under vacuum, leaving an oily yellow solid. The solid was extracted into pentane and filtered. The filtrate collected was a mixture of ~6:1 dimer (N2P2)/tetramer (N4P4) based on NMR (Figure S1), while the undissolved solid was mostly tetramer. The solvent of the filtrate was removed via vacuum to give a white solid as the crude product. The crude product can be further purified by another extraction in *n*-pentane to give the final product that contains at least 95% N2P2 (Figure S2). Yield: 488 mg, 73%.  $^1\text{H}$  NMR (300 MHz,  $(\text{CD}_3)_2\text{CO}$ )  $\delta$  (ppm): 1.23 (d,  $J = 13.1$  Hz, 18H, *t*-Bu), 6.73 (d,  $J = 7.8$  Hz, 4H, Py  $\text{H}_{\text{meta}}$ ), 7.81 (t,  $J = 7.8$  Hz, 2H, Py  $\text{H}_{\text{para}}$ ).  $^{13}\text{C}$  NMR (500 MHz,  $\text{CDCl}_3$ )  $\delta$  (ppm): 24.09 (*t*-Bu), 24.24 (*t*-Bu), 104.84 (Py), 141.64 (Py), 159.72 (Py).  $^{31}\text{P}$  NMR (500 MHz,  $\text{CDCl}_3$ )  $\delta$  (ppm): 159.69. ESI-MS ( $m/z$ ): 395.1304. Calculated for  $[\text{C}_{18}\text{H}_{24}\text{N}_2\text{O}_4\text{P}_2]\text{H}^+$ : 395.1290.

**Synthesis of (N2P2)NiBr<sub>2</sub> (1).** The complex was prepared under  $\text{N}_2$ . A solution of  $\text{Ni}(\text{DME})\text{Br}_2$  (21.2 mg, 0.068 mmol) was added to a solution of N2P2 (31 mg, 0.079 mmol) in DCM. The mixture turned dark red. After stirring for 1 h, the solution was filtered and concentrated for recrystallization by pentane diffusion. Black crystals formed, and the supernatant was removed. The resulting solid was washed with pentane and dried *in vacuo*. The product (N2P2)NiBr<sub>2</sub> was isolated as a black solid. Yield: 28 mg, 67%.  $^1\text{H}$  NMR ( $\text{CD}_3\text{CN}$ , 300 MHz),  $\delta$  (ppm): 1.51 (s, 18H, *t*-Bu), 6.79 (d, 8H, Py  $\text{H}_{\text{meta}}$ ), 7.82 (br, 2H, Py  $\text{H}_{\text{para}}$ ). Elemental analysis: found, C 34.35, H 4.06 N 4.00%. Calculated  $[\text{C}_{18}\text{H}_{26}\text{Br}_2\text{N}_2\text{NiO}_3\text{P}_2]$ , C 34.27, H 4.15, N 4.44%.

**Synthesis of [(N2P2)Ni(MeCN)<sub>2</sub>](SbF<sub>6</sub>)<sub>2</sub> (2).** The complex was prepared under  $\text{N}_2$ . A solution of  $\text{AgSbF}_6$  (76 mg, 0.221 mmol) was added to a solution of (N2P2)NiBr<sub>2</sub> (68 mg, 0.111 mmol) in MeCN. After stirring for 15 min, the mixture turned green and the solution was filtered and concentrated for recrystallization by ether diffusion. Green crystals formed, and the supernatant was removed. The

resulting solid was washed with ether and dried *in vacuo*. The product  $[(\text{N2P2})\text{Ni}(\text{MeCN})_2](\text{SbF}_6)_2$  was isolated as a green solid. Yield: 66 mg, 61%. Elemental analysis: found, C 26.27, H 2.93 N 5.70%. Calculated  $\text{C}_{22}\text{H}_{30}\text{F}_{12}\text{N}_4\text{NiO}_4\text{P}_2\text{Sb}_2$ , C 26.25, H 3.00, N 5.57%.

**Synthesis of [(N2P2)Ni(OTf)<sub>2</sub>] (3).** The complex was prepared under  $\text{N}_2$ . To a solution of (N2P2)NiBr<sub>2</sub> (15 mg, 0.024 mmol) in MeCN was added  $\text{AgOTf}$  (13 mg, 0.048 mmol). After stirring for 1 h, the solution turns green and was filtered and concentrated. Toluene was layered on the solution, and slow evacuation resulted in purple crystals. The crystals were washed with ether, and the isolated crystals were dried *in vacuo*. The product  $[(\text{N2P2})\text{Ni}(\text{OTf})_2]$  was isolated as a purple solid. Yield: 17 mg, 90%. Elemental analysis: found, C 31.76, H 2.88 N 3.48%. Calculated  $\text{C}_{20}\text{H}_{24}\text{F}_6\text{N}_2\text{NiO}_{10}\text{P}_2\text{S}_2$ , C 31.98, H 3.22, N 3.73%.

**Synthesis of [(N2P2)Ni(CN*t*-Bu)](SbF<sub>6</sub>)<sub>2</sub> (4).** The complex was prepared under  $\text{N}_2$ . Into a solution of  $[(\text{N2P2})\text{Ni}(\text{MeCN})_2](\text{SbF}_6)_2$  (42 mg, 0.0435 mmol) in MeCN, *t*-BuNC (4.9  $\mu\text{L}$ , 0.0435 mmol) was added. After stirring for 30 min, the solution turns a darker green and was filtered. Ether was added to the solution to crash out pink/purple crystals. The crystals were washed with ether, and the isolated crystals were dried *in vacuo*. The product  $[(\text{N2P2})\text{Ni}(\text{CN}t\text{-Bu})](\text{SbF}_6)_2$  was isolated as a pink solid. Yield: 33.6 mg, 77%.  $^1\text{H}$  NMR ( $\text{CD}_3\text{CN}$ , 300 MHz),  $\delta$  (ppm): 1.87 (s, 27H, *t*-Bu), 7.20 (d, 4H, Py  $\text{H}_{\text{meta}}$ ), 8.14 (br, 2H, Py  $\text{H}_{\text{para}}$ ). Elemental analysis: found, C 27.09, H 2.95 N 4.21%. Calculated  $\text{C}_{23}\text{H}_{33}\text{F}_{12}\text{N}_3\text{NiO}_4\text{P}_2\text{Sb}_2$ , C 27.41, H 3.30, N 4.17%.

**EPR Studies of the Ni<sup>I</sup> Species.** An EPR tube was charged with a solution of the Ni complex in 1:3 MeCN/PrCN (v/v) and immersed into liquid nitrogen. Another solution containing 1 equiv of chemical reductant in the same solvent mixture was quickly added, mixed, and frozen in the EPR tube. An initial EPR spectrum was taken at 77 K. The sample was then carefully warmed up for 10–30 s to allow the two layers to further mix, quickly refrozen, and the EPR spectrum was recorded. The warming up step was repeated if necessary.

**Low-Temperature UV–Vis Studies of the [(N2P2)Ni(CN*t*-Bu)]<sup>+</sup> (6) Complex.** A 5 mL aliquot of 4 (0.5 mM) in MeCN was prepared, and UV–vis spectra were recorded initially only for 4 and monitored immediately after addition of 1 equiv of  $\text{CoCp}_2$  in order to observe 6 in solution.

**X-ray Structure Determination.** Crystals of appropriate dimensions were mounted on MiTeGen cryoloops in random orientations. Preliminary examination and data collection were performed using a Bruker Kappa Apex II or SMART Apex II Charge Coupled Device (CCD) Detector system single-crystal X-ray diffractometers equipped with an Oxford Cryostream LT device. All data were collected using graphite monochromated  $\text{Mo K}\alpha$  radiation ( $\lambda = 0.71073$  Å) from a fine-focus sealed-tube X-ray source. Preliminary unit cell constants were determined with a set of 36 narrow frame scans. Typical data sets consist of combinations of  $\omega$  and  $\phi$  scan frames with typical scan width of 0.5 and counting time of 15–30 s/frame at a crystal to detector distance of 3.5–5.0 cm. The collected frames were integrated using an orientation matrix determined from the narrow frame scans. Apex II and SAINT software packages<sup>45</sup> were used for data collection and data integration. Analysis of the integrated data did not show any decay. Final cell constants were determined by global refinement of *xyz* centroids for the complete data set. The collected data were corrected for systematic errors using SADABS<sup>45</sup> based on the Laue symmetry using equivalent reflections. Crystal data and intensity data collection parameters as well as additional details of structure refinement are given in the Supporting Information. Structure solution and refinement were carried out using the SHELXTL-PLUS software package.<sup>46</sup> The structure was solved by direct methods or Patterson method and refined successfully in the space groups listed below. Full matrix least-squares refinement was carried out by minimizing  $\sum w(F_o^2 - F_c^2)^2$ . The non-hydrogen atoms were refined anisotropically to convergence.

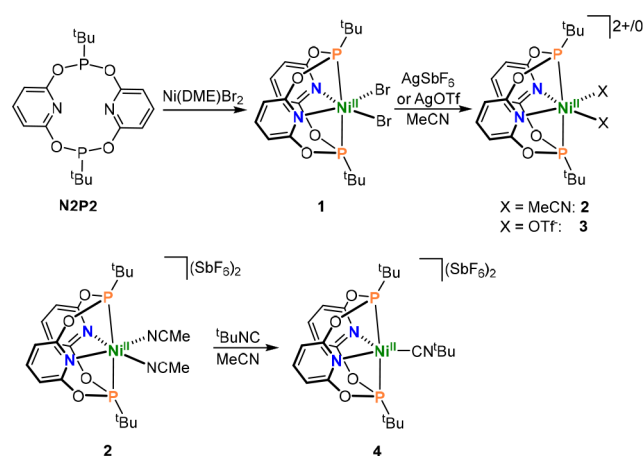
**General Procedure for the Kumada Cross-Coupling with (N2P2)NiBr<sub>2</sub>, 1.** Inside a nitrogen-filled glovebox, a small vial equipped with a magnetic stir bar was charged with the corresponding alkyl halide or aryl halide substrate (0.1 mmol), decane as internal

standard, and **1** (3 mg, 0.05 equiv) in THF (5.0 mL). To the stirring solution, the Grignard reagent (1.2 equiv) was added slowly over 1 h via syringe and the resulting solution was allowed to stir at room temperature for 24 h. At 1, 2, and 24 h an aliquot (500  $\mu$ L) was taken. Then, each reaction mixture was quenched with 5 mL of saturated  $\text{NH}_4\text{Cl}$  solution, extracted into diethyl ether (15 mL), and the organic layer was separated and dried over  $\text{MgSO}_4$ . The yield of product(s) was obtained by GC/FID using the internal standard for calibration and is an average of at least 3 independent runs, and the identity of the products was confirmed by GC/MSD.

## RESULTS AND DISCUSSION

**Synthesis and Structural Characterization of (N2P2) Ni Complexes 1–4.** Tetradentate diphosphonite pyridinophane ligand N2P2 was synthesized using modified procedures reported for noncyclic PNP pincer ligands.<sup>37,47–49</sup> The crude product was obtained as a mixture of the tetramer N4P4 and dimer N2P2 (Figure S1), and purification by multiple extractions into *n*-pentane yielded desired pure N2P2 (Figure S2).<sup>50</sup> The (N2P2)Ni<sup>II</sup> complexes 1–4 (Scheme 1) were

### Scheme 1. Synthesis of (N2P2)Ni<sup>II</sup> Complexes



synthesized in 60–90% yield by using common Ni<sup>II</sup> precursors and synthetic procedures. The complex (N2P2)NiBr<sub>2</sub> (**1**) was obtained through reaction of Ni(DME)Br<sub>2</sub> with 1 equiv of N2P2 in  $\text{CH}_2\text{Cl}_2$ /pentane. The complex [(N2P2)Ni(MeCN)<sub>2</sub>](SbF<sub>6</sub>)<sub>2</sub> (**2**) was conveniently synthesized by

bromide abstraction by 2 equiv of AgSbF<sub>6</sub> from (N2P2)NiBr<sub>2</sub> (**1**). The complex [(N2P2)Ni(OTf)<sub>2</sub>] (**3**) could not be synthesized by reacting Ni(OTf)<sub>2</sub> with N2P2, but instead, it was prepared through bromide abstraction by 2 equiv of AgOTf from **1**. The product obtained by the reaction of **2** with 1 equiv of *t*-BuNC in MeCN was found to be the monoisocyanide complex [(N2P2)Ni(CN*t*-Bu)](SbF<sub>6</sub>)<sub>2</sub> (**4**) in the solid state, according to single-crystal X-ray analysis (Figure 1). Interestingly, the addition of 2 equiv of *t*-BuNC did not yield the bisisocyanide complex, and instead it resulted in the decomposition of the complex, likely due to the loss of the N2P2 ligand. All complexes were isolated and purified by recrystallization and characterized by spectroscopic methods. The effective magnetic moments were measured in CDCl<sub>3</sub> for **1** and CD<sub>3</sub>CN for **2** and **3** at room temperature and their values were consistent with the expected value for a high-spin octahedral complex. Complexes **1**, **2**, and **3** each had a magnetic moment of 2.4  $\mu_B$ , 3.0  $\mu_B$ , and 2.3  $\mu_B$ , respectively. Complexes **1** and **2** were further characterized by elemental analysis.

X-ray quality crystals for complexes 1–4 were obtained by slow diffusion of pentane into concentrated solution of  $\text{CH}_2\text{Cl}_2$  for **1** and slow diffusion of Et<sub>2</sub>O into concentrated solutions in MeCN for **2**–**4**. The ORTEP plots and selected metrical parameters are given in Figure 1. The X-ray crystal structures of 1–3 reveal a distorted octahedral coordination at the Ni center, with the axial Ni–P bonds tilted toward the ligand (P–Ni–P = 148.9°, **1**; 150.46°, **2**; 152.04°, **3**). The average Ni–N bond lengths for 1–3 are 2.102, 2.080, and 2.054 Å, respectively. This trend of decreasing metal–ligand bond length is due to the decreasing strength of trans influence of the ligands (Br > MeCN > OTf). The X-ray crystal structure of **4** revealed a distorted trigonal bipyramidal coordination. Similar to 1–3, the axial Ni–P bonds tilt toward the ligand (P–Ni–P = 157.8°), albeit to a lesser extent given the reduced coordination number that leads to less steric repulsion.

**Electrochemical Studies.** The electrochemical properties of (N2P2)Ni<sup>II</sup> complexes were studied by CV (Table 1 and Figures S6–S9).<sup>50</sup> CV data of 1–4 in 0.1 M Bu<sub>4</sub>NClO<sub>4</sub>/MeCN show quasi-reversible redox waves for Ni<sup>I/II</sup> (Table 1 and Figures S6–S9). On the basis of these reduction potentials, complex **4** seems to be the easiest to be reduced, followed by **2**, **1**, and **3**, which is in line with the increasing

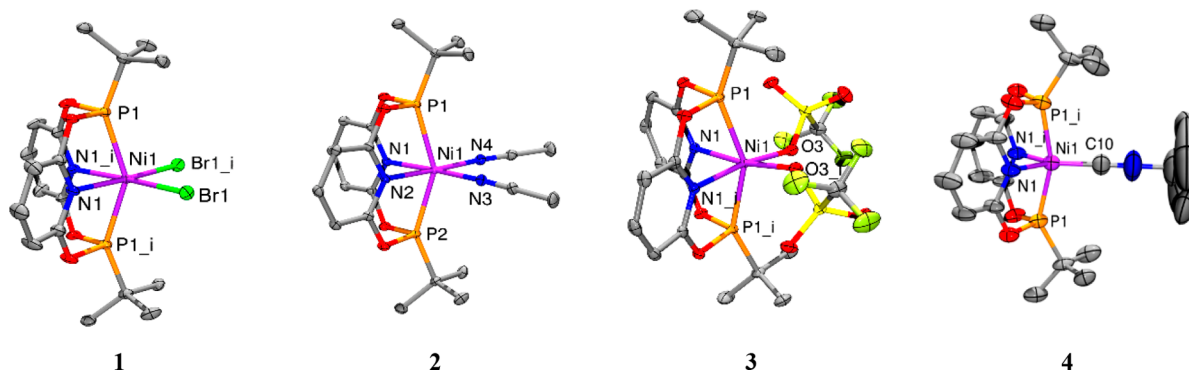


**Figure 1.** ORTEP representations (50% thermal ellipsoids) of the X-ray crystal structures of 1–4. Selected bond distances (Å): **1**, Ni1–Br1 = 2.4869(5), Ni1–Br1<sub>i</sub> = 2.4871(5), Ni1–N1 = 2.102(2), Ni1–N1<sub>i</sub> = 2.102(2), Ni1–P1 = 2.3138(8), Ni1–P1<sub>i</sub> = 2.3137(8); **2**, Ni1–N3 = 2.0374(13), Ni1–N4 = 2.0544(14), Ni1–N1 = 2.0881(12), Ni1–N2 = 2.0717(12), Ni1–P1 = 2.3271(4), Ni1–P2 = 2.3301(4); **3**, Ni1–O3 = 2.0429(14), Ni1–O3<sub>i</sub> = 2.0428(14), Ni1–N1 = Ni1 = N1<sub>i</sub> = 2.0535(16), Ni1–P1 = Ni1–P1<sub>i</sub> = 2.3140(5); **4**, Ni1–C10 = 1.80(2), Ni1–N1 = Ni1–N1<sub>i</sub> = 1.963(9), Ni1–P1 = Ni1–P1<sub>i</sub> = 2.145(3).

**Table 1. Cyclic Voltammetry (CV) Data for (N2P2)Ni Complexes**

complex	1	2	3	4
$E_{1/2}^{I/II}$ , V <sup>a</sup>	-0.875	-0.750	-1.170	-0.630
$\Delta E$ , mV	150	220	140	220

<sup>a</sup> $E_{1/2}^{I/II}$ , V ( $\Delta E_p$ , mV);  $E_{pa}$  values reported vs Fc at room temperature, 100 mV/s scan rate.

charge of the Ni<sup>II</sup> complex and the soft nature of the CN*t*-Bu ligand.

**Electron Paramagnetic Resonance (EPR) Studies.** The one-electron reduction of complex 3 was carried out by chemical reduction with 1 equiv of cobaltocene (CoCp<sub>2</sub>) to generate the Ni<sup>I</sup> species [(N2P2)Ni<sup>I</sup>(OTf)(MeCN)] (5). The EPR spectrum (77K, 1:3 MeCN/PrCN glass) of 5 reveals a pseudo-axial signal corresponding to a Ni<sup>I</sup>, d<sup>9</sup> metal center with a  $S = 1/2$  ground state where the unpaired electron has predominant d<sub>z<sup>2</sup></sub> character and  $g_{ave} = 2.05940$  (Figure 2). The

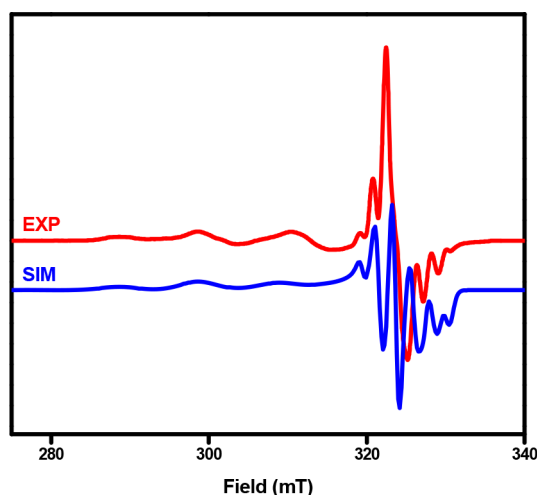


**Figure 2.** EPR spectrum (red line) of [(N2P2)Ni<sup>I</sup>(OTf)(MeCN)] (5) in 3:1 PrCN/MeCN glass at 77 K, and the simulated EPR spectrum (blue line) using the following parameters:  $g_x = 2.007$  ( $A_{2P} = 21$  G;  $A_{1N} = 22$  G),  $g_y = 1.994$  ( $A_{2P} = 11$  G;  $A_{1N} = 33$  G),  $g_z = 2.177$  ( $A_{2P} = 100$  G;  $A_{1N} = 10$  G). Frequency: 9096.337 MHz.

EPR spectrum revealed superhyperfine coupling ( $A_{2P} = 11$ – $100$  G,  $I = 1/2$ ) to the two axial P donors, and also to the single equatorial N donor ( $A_{1N} = 10$ – $33$  G,  $I = 1$ ). It is expected that in solution the triflate anions can be replaced by MeCN solvent molecules, which will provide the N atom that can undergo superhyperfine coupling to the Ni<sup>I</sup> center. Thus, we propose the formation of a 5- or 4-coordinate [(N2P2)-Ni<sup>I</sup>(MeCN)]<sup>+</sup> species in solution, with the N2P2 ligand bound in a  $\kappa^3$  or  $\kappa^4$  conformation.

One-electron reduction of complex 4 was also carried out by chemical reduction with 1 equiv of CoCp<sub>2</sub> to generate the Ni<sup>I</sup> species [(N2P2)Ni<sup>I</sup>(CN*t*-Bu)]<sup>+</sup> (6). The EPR spectrum (77K, 1:3 MeCN:PrCN glass) of 6 reveals a rhombic signal corresponding to a Ni<sup>I</sup>, d<sup>9</sup> metal center with an  $S = 1/2$  ground state where the unpaired electron has predominant d<sub>z<sup>2</sup></sub> character and  $g_{ave} = 2.0585$  (Figure 3a). The EPR spectrum revealed strong superhyperfine coupling ( $A_{2P} = 182$ – $199$  G,  $I = 1/2$ ) to the two axial P donors, suggesting an appreciable delocalization of the unpaired electron onto the phosphorus atoms of the N2P2 ligand, as supported by the DFT-calculated

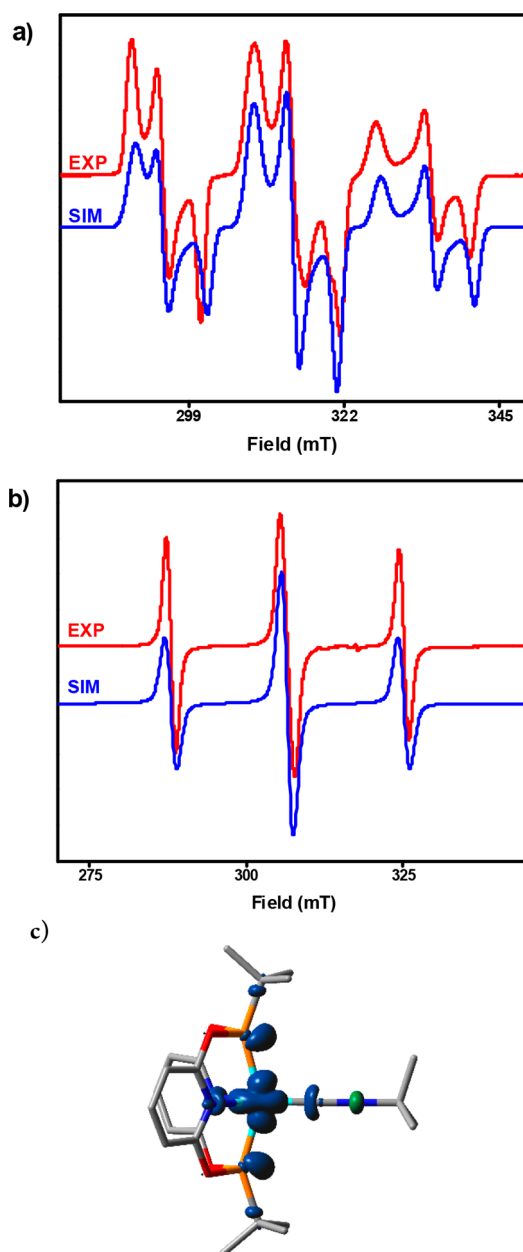


**Figure 3.** (a) EPR spectrum (red line) of [(N2P2)Ni(CN*t*-Bu)](SbF<sub>6</sub>) (6) in 3:1 PrCN:MeCN glass, 77 K, and the simulated EPR spectrum (blue line) using the following parameters:  $g_x = 2.098$  ( $A_{2P} = 182$  G),  $g_y = 2.060$  ( $A_{2P} = 199$  G),  $g_z = 2.017$  ( $A_{2P} = 198$  G). Frequency: 9092.747 MHz. (b) EPR spectrum (red line) of [(N2P2)Ni(CN*t*-Bu)](SbF<sub>6</sub>) (6) in 3:1 PrCN:MeCN glass, room temperature, and the simulated EPR spectrum (blue line) using the following parameters:  $g_{ave} = 2.070$  ( $A_{2P} = 186$  G). Frequency: 8879.542 MHz. (c) DFT-calculated spin density for 6, shown as a 0.03 isodensity contour plot.

spin density plot (Figure 3c). Similarly, large phosphorus coupling ranging from 18–31 G has been reported for nickel complexes stabilized by PCP pincer ligand, where Kozhanov et al. speculates that the phosphorus coupling reflects the amount of contribution from a group metal–pincer orbital to the orbital containing the unpaired electron.<sup>51,52</sup> Therefore, the strong accepting *t*-BuNC ligand leads to a greater superhyperfine coupling constant versus the OTf or MeCN ligands in 5. The stronger interaction with the P atoms could also lead

to a preferred trigonal bipyramidal geometry for this Ni<sup>I</sup> species.

The Ni<sup>I</sup> EPR of **6** can be observed for up to 1 h at room temperature, although at 45 min the signal has decreased significantly (>80%). A room-temperature EPR (298 K, 1:3 MeCN/PrCN glass) was also prepared where the sample prepared at low-temperature was quickly thawed to room temperature and was immediately put into the instrument. The room temperature EPR also revealed strong superhyperfine coupling ( $A_{2p} = 185.8$  G) to the two P donors with  $g = 2.06992$  (Figure 3b).

**Isolation of the (N2P2)Ni<sup>I</sup> Complex 6.** The surprising stability of **6** allowed for its isolation. Into a solution of **4**, 1 equiv of CoCp<sub>2</sub> was added at  $-70$  °C, and the solution was stirred for 30 min as its color changed from pink to purple. The dark purple solution was filtered, and a dark purple solid was precipitated using diethyl ether. The resulting solid was dried *in vacuo*, and the product of a Ni<sup>I</sup> species was confirmed via EPR. While X-ray quality crystals of **6** could not be obtained despite several attempts, the complex was further analyzed by X-ray photoelectron spectroscopy (XPS). The resulting XPS spectrum shows a decrease in the Ni 2p<sub>3/2</sub> and 2p<sub>1/2</sub> binding energies of  $\sim 1.39$  eV between **4** and **6** and is consistent with the presence of a more reduced Ni center in **6** versus **4** (Figure 4).<sup>53</sup>

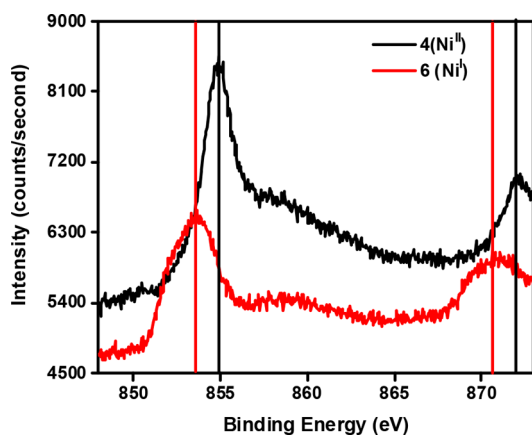


**Figure 4.** X-ray photoelectron spectra of the Ni binding energy region for complexes **4** (black line) and **6** (red line). Selected binding energies (eV): **4**: 2p<sub>3/2</sub>, 854.88; 2p<sub>1/2</sub>, 872.18; **6**: 2p<sub>3/2</sub>, 853.66; 2p<sub>1/2</sub>, 870.94.

To further probe the formation of a Ni<sup>I</sup> species, the reduction reaction of **4** to yield **6** was carried out in MeCN at low temperature and monitored by UV–vis spectroscopy. The spectrum reveals two bands at 543 and 468 nm that appear after the addition of CoCp<sub>2</sub> at  $-45$  °C, followed by their decay during the next few minutes as the cell was warmed to room temperature (Figure 5a). The time-dependent density functional theory (TD-DFT) calculated UV–vis spectrum and transitions of **6** show similar transitions to the experimental spectrum (Figure 5b) providing support for the proposed trigonal bipyramidal geometry of **6** with N2P2 ligand binding in a  $\kappa^4$  conformation.

Further insight into the electronic properties of **6** was obtained by DFT calculations. The geometry optimized structure of **6** reveals a Ni<sup>I</sup> center in a trigonal bipyramidal geometry that adopts an  $S = 1/2$  ground state in which the

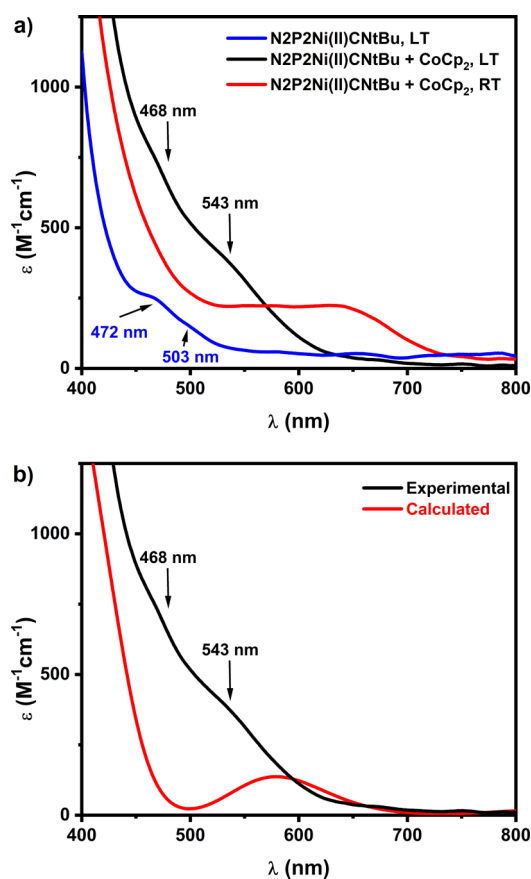


**Figure 5.** (a) *In situ* UV–vis spectra of the reduction of **4** (0.5 mM, black line) with 1 equiv of CoCp<sub>2</sub> in MeCN at  $-45$  °C: (blue line) initial spectrum before adding CoCp<sub>2</sub> at  $-45$  °C; (red line) spectrum at room temperature after adding CoCp<sub>2</sub>. (b) Experimental and normalized calculated TD-DFT UV–vis spectrum of **6**.

unpaired electron has predominant  $d_{z^2}$  character (Figure 3c), in line with the observed EPR spectrum.

**Kumada Cross-Coupling Reactivity.** Since the CV studies revealed that **1** can be oxidized and reduced *in situ* to the Ni<sup>III</sup> and Ni<sup>I</sup> species, respectively (Figure S6),<sup>50</sup> we proposed that **1** may be an active catalyst for the Kumada cross-coupling of aryl iodides with aryl or alkyl Grignard reagents. Excitingly, the reaction of iodotoluene with phenylmagnesium bromide or 1-hexylmagnesium bromide affords the corresponding coupled products in 99 and 95% unoptimized yields, respectively (Scheme 2). By contrast, a lower yield of

#### Scheme 2. Kumada Cross-Coupling Reactions Catalyzed by **1**<sup>a</sup>

$$\text{R-X} + \text{R}'\text{-MgBr} \xrightarrow[\text{THF, RT}]{5\% (\text{N2P2})\text{NiBr}_2} \text{R-R}'$$

R-X	R'MgX	Reaction time, h	Yield, %
p-tolyl-I	phenylMgBr	1	95
p-tolyl-I	hexylMgBr	1	95
octyl-I	hexylMgBr	1	17

<sup>a</sup>Yields were determined using GC-FID with decane as the internal standard; no coupled products were observed in the absence of **1**.

17% was observed for the reaction of octyl-iodide with hexylMgBr, while the reaction of chlorotoluene with phenyl-magnesium bromide gave the coupled product in 41% only.<sup>50</sup> Similar results were observed recently using (<sup>Me</sup>N4)NiMe<sub>2</sub> complex,<sup>36</sup> but we were pleasantly surprised to see complex 1 had a yield (95%) for the cross-coupling reaction with hexylMgBr much higher than the 60% yield observed with the (<sup>Me</sup>N4)NiMe<sub>2</sub> complex. Further mechanistic studies are in progress to further probe the catalytic reactivity of these (N2P2)Ni complexes.

## CONCLUSION

In conclusion, herein we have reported the use of a novel N- and P-donor ligand, *P,P'*-ditertbutyl-2,11-diphosphonito[3.3]-(2,6)pyridinophane (N2P2), to stabilize various Ni complexes and study their electronic properties and reactivity. Interestingly, a Ni<sup>I</sup> complex [(N2P2)Ni(CN*t*-Bu)](SbF<sub>6</sub>) was isolated and characterized by EPR and XPS. In addition, the (N2P2)NiBr<sub>2</sub> complex was shown to be a competent catalyst in Kumada cross-coupling reactions. Overall, the newly developed N2P2 ligand provides P donor atoms to interact with the Ni centers and thus stabilize low-valent Ni species, in contrast to the all-N donor N4-type ligands. Thus, the redox reactivity of the various (N2P2)Ni complexes is expected to be far-reaching and is currently being further explored for other catalytic and electrocatalytic applications.

## ASSOCIATED CONTENT

### Supporting Information

The Supporting Information is available free of charge at <https://pubs.acs.org/doi/10.1021/acs.organomet.1c00003>.

Cyclic voltammograms, ESI-MS spectra, EPR simulation details, <sup>1</sup>H NMR spectra, X-ray crystallographic data, and computational details (PDF)

### Accession Codes

CCDC 2049806–2049809 contain the supplementary crystallographic data for this paper. These data can be obtained free of charge via [www.ccdc.cam.ac.uk/data\\_request/cif](http://www.ccdc.cam.ac.uk/data_request/cif), or by emailing [data\\_request@ccdc.cam.ac.uk](mailto:data_request@ccdc.cam.ac.uk), or by contacting The Cambridge Crystallographic Data Centre, 12 Union Road, Cambridge CB2 1EZ, UK; fax: +44 1223 336033.

## AUTHOR INFORMATION

### Corresponding Author

Liviu M. Mirica – Department of Chemistry, University of Illinois at Urbana–Champaign, Urbana, Illinois 61801, United States; [orcid.org/0000-0003-0584-9508](https://orcid.org/0000-0003-0584-9508); Email: [mirica@illinois.edu](mailto:mirica@illinois.edu)

### Authors

Kei Fuchigami – Department of Chemistry, Washington University, St. Louis, Missouri 63130-4899, United States  
Michael B. Watson – Department of Chemistry, Washington University, St. Louis, Missouri 63130-4899, United States  
Giang N. Tran – Department of Chemistry, University of Illinois at Urbana–Champaign, Urbana, Illinois 61801, United States  
Nigam P. Rath – Department of Chemistry and Biochemistry, University of Missouri–St. Louis, St. Louis, Missouri 63121-4400, United States

Complete contact information is available at:

<https://pubs.acs.org/doi/10.1021/acs.organomet.1c00003>

## Notes

The authors declare no competing financial interest.

## ACKNOWLEDGMENTS

We thank the Department of Energy's BES Catalysis Science Program (DE-SC0006862) for financial support. We thank Sagnik Chakrabarti for assistance with the synthesis of N2P2 and Bailey Bouley with the refinement of the X-ray structure of 4.

## REFERENCES

- (1) Devasagayaraj, A.; Studemann, T.; Knochel, P. A new nickel-catalyzed cross-coupling reaction between sp(3) carbon centers. *Angew. Chem., Int. Ed. Engl.* **1996**, *34*, 2723.
- (2) Netherton, M. R.; Fu, G. C. Nickel-catalyzed cross-couplings of unactivated alkyl halides and pseudohalides with organometallic compounds. *Adv. Synth. Catal.* **2004**, *346*, 1525.
- (3) Frisch, A. C.; Beller, M. Catalysts for cross-coupling reactions with non-activated alkyl halides. *Angew. Chem., Int. Ed.* **2005**, *44*, 674.
- (4) Terao, J.; Kambe, N. Cross-Coupling Reaction of Alkyl Halides with Grignard Reagents Catalyzed by Ni, Pd, or Cu Complexes with pi-Carbon Ligand(s). *Acc. Chem. Res.* **2008**, *41*, 1545.
- (5) Glorius, F. Asymmetric Cross-Coupling of Non-Activated Secondary Alkyl Halides. *Angew. Chem., Int. Ed.* **2008**, *47*, 8347.
- (6) Rudolph, A.; Lautens, M. Secondary Alkyl Halides in Transition-Metal-Catalyzed Cross-Coupling Reactions. *Angew. Chem., Int. Ed.* **2009**, *48*, 2656.
- (7) Phapale, V. B.; Cardenas, D. J. Nickel-catalyzed Negishi cross-coupling reactions: scope and mechanisms. *Chem. Soc. Rev.* **2009**, *38*, 1598.
- (8) Hu, X. Nickel-catalyzed cross coupling of non-activated alkyl halides: a mechanistic perspective. *Chem. Sci.* **2011**, *2*, 1867.
- (9) Knochel, P.; Thaler, T.; Diene, C. Pd-, Ni-, Fe-, and Co-Catalyzed Cross-Couplings Using Functionalized Zn-, Mg-, Fe-, and In-Organometallics. *Isr. J. Chem.* **2010**, *50*, 547.
- (10) Tasker, S. Z.; Standley, E. A.; Jamison, T. F. Recent advances in homogeneous nickel catalysis. *Nature* **2014**, *509*, 299.
- (11) Tsou, T. T.; Kochi, J. K. Reductive Coupling of Organometals Induced by Oxidation - Detection of Metastable Paramagnetic Intermediates. *J. Am. Chem. Soc.* **1978**, *100*, 1634.
- (12) Tsou, T. T.; Kochi, J. K. Mechanism of biaryl synthesis with nickel complexes. *J. Am. Chem. Soc.* **1979**, *101*, 7547.
- (13) Amatore, C.; Jutand, A. Rates and mechanism of biphenyl synthesis catalyzed by electrogenerated coordinatively unsaturated nickel complexes. *Organometallics* **1988**, *7*, 2203.
- (14) Matsunaga, P. T.; Hillhouse, G. L.; Rheingold, A. L. Oxygen-atom transfer from nitrous oxide to a nickel metallacycle - synthesis, structure, and reactions of (2,2'-bipyridine)Ni(OCH<sub>2</sub>CH<sub>2</sub>CH<sub>2</sub>CH<sub>2</sub>). *J. Am. Chem. Soc.* **1993**, *115*, 2075.
- (15) Koo, K. M.; Hillhouse, G. L.; Rheingold, A. L. Oxygen-Atom Transfer from Nitrous-Oxide to an Organonickel(II) Phosphine Complex - Syntheses and Reactions of New Nickel(II) Aryloxides and the Crystal-Structure of (Me(2)Pch(2)Ch(2)Pme(2))Ni(O-O-C(6)-H(4)Cme(2)Ch(2)). *Organometallics* **1995**, *14*, 456.
- (16) Lin, B. L.; Clough, C. R.; Hillhouse, G. L. Interactions of aziridines with nickel complexes: Oxidative-addition and reductive-elimination reactions that break and make C-N bonds. *J. Am. Chem. Soc.* **2002**, *124*, 2890.
- (17) Jones, G. D.; McFarland, C.; Anderson, T. J.; Vicic, D. A. Analysis of key steps in the catalytic cross-coupling of alkyl electrophiles under Negishi-like conditions. *Chem. Commun.* **2005**, 4211.
- (18) Klein, A.; Budnikova, Y. H.; Sinyashin, O. G. Electron transfer in organonickel complexes of  $\alpha$ -diimines: Versatile redox catalysts for C-C or C-P coupling reactions - A review. *J. Organomet. Chem.* **2007**, *692*, 3156.
- (19) Iluc, V. M.; Miller, A. J. M.; Anderson, J. S.; Monreal, M. J.; Mehn, M. P.; Hillhouse, G. L. Synthesis and Characterization of

Three-Coordinate Ni(III)-Imide Complexes. *J. Am. Chem. Soc.* **2011**, *133*, 13055.

(20) Yu, S.; Dudkina, Y.; Wang, H.; Kholin, K. V.; Kadirov, M. K.; Budnikova, Y. H.; Vicic, D. A. Accessing perfluoroalkyl nickel(ii), (iii), and (iv) complexes bearing a readily attached [C4F8] ligand. *Dalton Trans.* **2015**, *44*, 19443.

(21) Mohadjer Beromi, M.; Banerjee, G.; Brudvig, G. W.; Hazari, N.; Mercado, B. Q. Nickel(I) Aryl Species: Synthesis, Properties, and Catalytic Activity. *ACS Catal.* **2018**, *8*, 2526.

(22) Dicciani, J. B.; Diao, T. Mechanisms of Nickel-Catalyzed Cross-Coupling Reactions. *Trends Chem.* **2019**, *1*, 830.

(23) Dicciani, J. B.; Katigbak, J.; Hu, C.; Diao, T. Mechanistic Characterization of (Xantphos)Ni(I)-Mediated Alkyl Bromide Activation: Oxidative Addition, Electron Transfer, or Halogen-Atom Abstraction. *J. Am. Chem. Soc.* **2019**, *141*, 1788.

(24) Dicciani, J.; Lin, Q.; Diao, T. Mechanisms of Nickel-Catalyzed Coupling Reactions and Applications in Alkene Functionalization. *Acc. Chem. Res.* **2020**, *53*, 906.

(25) Somerville, R. J.; Odena, C.; Obst, M. F.; Hazari, N.; Hopmann, K. H.; Martin, R. Ni(I)-Alkyl Complexes Bearing Phenanthroline Ligands: Experimental Evidence for CO<sub>2</sub> Insertion at Ni(I) Centers. *J. Am. Chem. Soc.* **2020**, *142*, 10936.

(26) Khusnutdinova, J. R.; Rath, N. P.; Mirica, L. M. Stable Mononuclear Organometallic Pd(III) Complexes and Their C-C Bond Formation Reactivity. *J. Am. Chem. Soc.* **2010**, *132*, 7303.

(27) Khusnutdinova, J. R.; Rath, N. P.; Mirica, L. M. The Aerobic Oxidation of a Pd(II) Dimethyl Complex Leads to Selective Ethane Elimination from a Pd(III) Intermediate. *J. Am. Chem. Soc.* **2012**, *134*, 2414.

(28) Tang, F.; Zhang, Y.; Rath, N. P.; Mirica, L. M. Detection of Pd(III) and Pd(IV) Intermediates during the Aerobic Oxidative C-C Bond Formation from a Pd(II) Dimethyl Complex. *Organometallics* **2012**, *31*, 6690.

(29) Tang, F.; Qu, F.; Khusnutdinova, J. R.; Rath, N. P.; Mirica, L. M. Structural and Reactivity Comparison of Analogous Organometallic Pd(III) and Pd(IV) Complexes. *Dalton Trans.* **2012**, *41*, 14046.

(30) Mirica, L. M.; Khusnutdinova, J. R. Structure and Electronic Properties of Pd(III) Complexes. *Coord. Chem. Rev.* **2013**, *257*, 299.

(31) Zheng, B.; Tang, F.; Luo, J.; Schultz, J. W.; Rath, N. P.; Mirica, L. M. Organometallic Nickel(III) Complexes Relevant to Cross-Coupling and Carbon-Heteroatom Bond Formation Reactions. *J. Am. Chem. Soc.* **2014**, *136*, 6499.

(32) Zhou, W.; Schultz, J. W.; Rath, N. P.; Mirica, L. M. Aromatic Methoxylation and Hydroxylation by Organometallic High-Valent Nickel Complexes. *J. Am. Chem. Soc.* **2015**, *137*, 7604.

(33) Tang, F. Z.; Rath, N. P.; Mirica, L. M. Stable bis-(trifluoromethyl)nickel(III) complexes. *Chem. Commun.* **2015**, *51*, 3113.

(34) Zhou, W.; Rath, N. P.; Mirica, L. M. Oxidatively-induced aromatic cyanation mediated by Ni(III). *Dalton Trans.* **2016**, *45*, 8693.

(35) Zhou, W.; Zheng, S. A.; Schultz, J. W.; Rath, N. P.; Mirica, L. M. Aromatic Cyanoalkylation through Double C-H Activation Mediated by Ni(III). *J. Am. Chem. Soc.* **2016**, *138*, 5777.

(36) Schultz, J. W.; Fuchigami, K.; Zheng, B.; Rath, N. P.; Mirica, L. M. Isolated Organometallic Nickel(III) and Nickel(IV) Complexes Relevant to Carbon-Carbon Bond Formation Reactions. *J. Am. Chem. Soc.* **2016**, *138*, 12928.

(37) Bernskoetter, W. H.; Hanson, S. K.; Buzak, S. K.; Davis, Z.; White, P. S.; Swartz, R.; Goldberg, K. I.; Brookhart, M. Investigations of Iridium-Mediated Reversible C-H Bond Cleavage: Characterization of a 16-Electron Iridium(III) Methyl Hydride Complex. *J. Am. Chem. Soc.* **2009**, *131*, 8603.

(38) Bernskoetter, W. H.; Schauer, C. K.; Goldberg, K. I.; Brookhart, M. Characterization of a Rhodium(I) sigma-Methane Complex in Solution. *Science* **2009**, *326*, 553.

(39) Salem, H.; Shimon, L. J. W.; Diskin-Posner, Y.; Leitus, G.; Ben-David, Y.; Milstein, D. Formation of Stable trans-Dihydride

Ruthenium(II) and 16-Electron Ruthenium(0) Complexes Based on Phosphinite PONOP Pincer Ligands. Reactivity toward Water and Electrophiles. *Organometallics* **2009**, *28*, 4791.

(40) Findlater, M.; Bernskoetter, W. H.; Brookhart, M. Proton-Catalyzed Hydrogenation of a d8 Ir(I) Complex Yields a trans Ir(III) Dihydride. *J. Am. Chem. Soc.* **2010**, *132*, 4534.

(41) Kundu, S.; Brennessel, W. W.; Jones, W. D. Synthesis and Reactivity of New Ni, Pd, and Pt 2,6-Bis(di-tert-butylphosphinito)-pyridine Pincer Complexes. *Inorg. Chem.* **2011**, *50*, 9443.

(42) Boudier, A.; Breuil, P.-A. R.; Magna, L.; Olivier-Bourbigou, H.; Braunstein, P. Nickel(II) complexes with imino-imidazole chelating ligands bearing pendant donor groups (SR, OR, NR<sub>2</sub>, PR<sub>2</sub>) as precatalysts in ethylene oligomerization. *J. Organomet. Chem.* **2012**, *718*, 31.

(43) Evans, D. F. The determination of the paramagnetic susceptibility of substances in solution by nuclear magnetic resonance. *J. Chem. Soc.* **1959**, 2003.

(44) De Buysser, K.; Herman, G. G.; Bruneel, E.; Hoste, S.; Van Driessche, I. Determination of the Number of Unpaired Electrons in Metal-Complexes. A Comparison Between the Evans' Method and Susceptometer Results. *Chem. Phys.* **2005**, *315*, 286.

(45) Bruker Analytical X-Ray; Bruker: Madison, WI, 2010.

(46) Sheldrick, G. A short history of SHELX. *Acta Crystallogr., Sect. A: Found. Crystallogr.* **2008**, *64*, 112.

(47) Hermann, D.; Gandelman, M.; Rozenberg, H.; Shimon, L. J. W.; Milstein, D. Synthesis, structure, and reactivity of new rhodium and iridium complexes, bearing a highly electron-donating PNP system. Iridium-mediated vinylic C-H bond activation. *Organometallics* **2002**, *21*, 812.

(48) Rubio, M.; Suárez, A.; Vega, E.; Álvarez, E.; Díez, J.; Gamasa, M. P.; Pizzano, A. Synthesis and Structural Characterization of Pincer Pyridine Diphosphite Complexes of Rhodium and Iridium. *J. Inorg. Chem.* **2012**, *2012*, 655.

(49) Kundu, S.; Brennessel, W. W.; Jones, W. D. Synthesis and Reactivity of New Ni, Pd, and Pt 2,6-Bis(di-tert-butylphosphinito)-pyridine Pincer Complexes. *Inorg. Chem.* **2011**, *50*, 9443.

(50) See the Supporting Information.

(51) Kozhanov, K. A.; Bubnov, M. P.; Cherkasov, V. K.; Fukin, G. K.; Abakumov, G. A. EPR study of intramolecular dynamics in o-semiquinonic nickel complexes with PCP-pincer ligand in solution. *Dalton Trans.* **2004**, 2957.

(52) Nevodchikov, V. I.; Abakumov, G. A.; Cherkasov, V. K.; Razuvaev, G. A. ESR investigation of the substitution reactions in rhodium(I) complexes with spin-labeled ligands. *J. Organomet. Chem.* **1981**, *214*, 119.

(53) Moulder, J. F.; Stickle, W. F.; Sobol, P. E.; Bomben, K. D. *Handbook of X-ray Photoelectron Spectroscopy: A Reference Book of Standard Spectra for Identification and Interpretation of XPS Data*; Perkin-Elmer: Eden Prairie, MN, 1992.